CHEMISTRY
A EUROPEAN JOURNAL

DOI: 10.1002/chem.201102032

Controlling Conformations in Alternating Dialkylsilylene-Spaced Donor–Acceptor Copolymers by a Cooperative Thorpe–Ingold Effect and Polymer Folding

Chih-Hsien Chen,[a] Yen-Chin Huang,[a] Wei-Chih Liao,[a] Tsong-Shin Lim,[b] Kuan-Lin Liu,[c] I-Chia Chen,[c] and Tien-Yau Luh*[a]

Dedicated to Professor Leon M. Stock on the occasion of his 80th birthday

Abstract: A series of dialkylsilylene-spaced copolymers **6** and **7**, which contain Me_2Si and iPr_2Si spacer groups, respectively, and have alternating donor and acceptor chromophores, have been designed and regioselectively synthesized by hydrosilylation. The ratio of the donor and acceptor chromophores for each repeat unit is 2:1, and the two donor chromophores are linked by a trimethylene bridge. A 4-aminostyrene moiety is used as the donor and a series of acceptor chromophores with different reduction potentials are employed. Both steady-state and kinetic measurements reveal that the photoinduced electron transfer (PET) in **6** obeyed the Marcus theory in which normal and inverted regions are observed. On the other hand, the iPr_2Si-spaced copolymers **7** exhibit absorption and emission from the charge-transfer complexes exclusively due to ground-state interactions between the donor and acceptor chromophores. The discrepancy in photophysical behavior may have arisen from the difference in distance between the adjacent donor and acceptor chromophores. The bulkiness of the substituents on the silicon atom (i.e., Me versus *i*Pr) may exert the Thorpe–Ingold effect on the local conformation around the silicon atom. The differences in the small energetic barriers for each of the conformational states may be amplified by extending the distance of the folding structure, which results in perturbing the conformation of the polymers. These results suggest that the electronic interactions between adjacent donor–acceptor pairs in these copolymers are controlled by the synchronization of the substitution effect and corresponding polymeric structures.

Keywords: Marcus theory · photoinduced electron transfer · polymer folding · silicon · substituted silylene · Thorpe–Ingold effect

Introduction

Polymer folding represents, among other things, an ensemble of rotation about the sigma bonds along the polymeric backbones, through-space electrostatic and steric interactions between non-neighboring sites, and solvophobic effects.[1–8] The differences in the small energetic barriers for each of the conformational states may be amplified by extending the distance of the folding structure, which results in a more stable conformation.[8] Numerous secondary structures of polymers[3,4] and proteins[5,6] are known to be stabilized by hydrogen bonding. Also, π–π stacking interactions play an important role in the folding and intermolecular aggregation/assembly of a polymer.[7] Circular dichroism, fluorescence quenching, and excimer formation have frequently been used as probes for the folding of macromolecules.[9,10] Nevertheless, knowledge of the precise conformational arrangement of artificial polymers remains a challenging problem, especially for subnanometric variations in folded structures. Photoinduced electron transfer (PET) has been known to be sensitive to subtle changes in distance on the angstrom scale.[11] In other words, electronic coupling between the donor and acceptor is strongly perturbed by a slight variation in the distance between the chromophores.[12] Indeed, the use of this strategy for investigation of protein conformation has been carried out.[13] It is envisaged that the use of PET as a probe might also provide information about the fine structures of folded polymers.

Monosilylene-spaced copolymers **1**[14] are known to exhibit extraordinary photophysical properties;[15–18] furthermore, different aryl groups (i.e., Ar^1 and Ar^2) can be regioselectively incorporated in the polymer chain by using a simple hydrosilylation protocol. The silicon moiety in **1**, in general,

[a] Dr. C.-H. Chen, Y.-C. Huang, W.-C. Liao, Prof. T.-Y. Luh
Department of Chemistry
National Taiwan University
Taipei, 106 (Taiwan)
Fax: (+886)223644971
E-mail: tyluh@ntu.edu.tw

[b] Prof. T.-S. Lim
Department of Physics
Tunghai University
Taichung, 407 (Taiwan)

[c] K.-L. Liu, Prof. I.-C. Chen
Department of Chemistry
National Tsing Hua University
Hsinchu, 300 (Taiwan)

Supporting information for this article is available on the WWW under http://dx.doi.org/10.1002/chem.201102031.

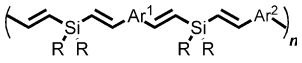

1

is considered to be an insulating tetrahedral spacer.[14–19] Thus, the electronic interactions between chromophores can be simplified in comparison with conjugated polymers. Moreover, the steric nature of the substituents on the silicon atom can have a bearing on the morphological changes.[20] Such a small variation might fine-tune the features of the ensembled polymers that originate from the conformational equilibrium of divinylsilane moiety in **1** due to the Thorpe–Ingold effect [Eq. (1)]. Accordingly, we chose monosilylene-spaced copolymer **1** as a skeleton to study the conformational change of the polymeric structure by utilizing the features of the PET process in polymers.

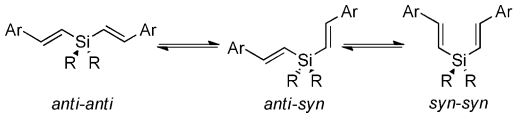

anti-anti anti-syn syn-syn (1)

Results and Discussion

Strategy: To decrease the complexity of conformational changes in **1**, one of the two vinyl moieties in **1** was replaced by an aryl group so that the equilibrium shown in Equation (1) could be simplified to Equation (2), in which only *syn* and *anti* equilibrium will be considered.

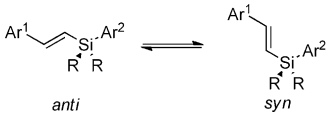

anti syn (2)

Aromatic amines are widely used as electron donors in PET reactions.[21] Because of synthetic convenience, we decided to use two donors symmetrically located at both ends of the acceptor chromophore. First, model compounds **2** and **3** were synthesized,[22] in which the aminostyrene group was employed as the donor and the stilbene moiety as the acceptor. The absorption spectra for **2** and **3** were almost identical (Figure 1). Both **2** and **3** exhibit dual emission bands at $\lambda = 380$ nm due to intrinsic local excited (LE) emission of the stilbene chromophore and at $\lambda = 500$ nm which are likely to belong to the emission from the charge-separation state (CT emission; Figure 1). It is interesting to note that the relative intensity of the LE appeared to be much lower in **3** with two donor chromophores than in **2**, which has only one donor chromophore. In addition, the relative intensity of the CT emission was much higher in **3** than in **2**. Accordingly, PET would be more efficient in **3** than in **2**.

Oligomethylene bridges were designed to link two aminostyrene chromophores. To test the effect of the chain length

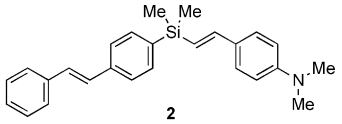

2

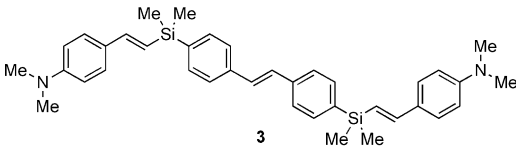

3

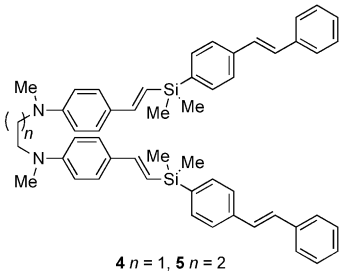

4 $n = 1$, **5** $n = 2$

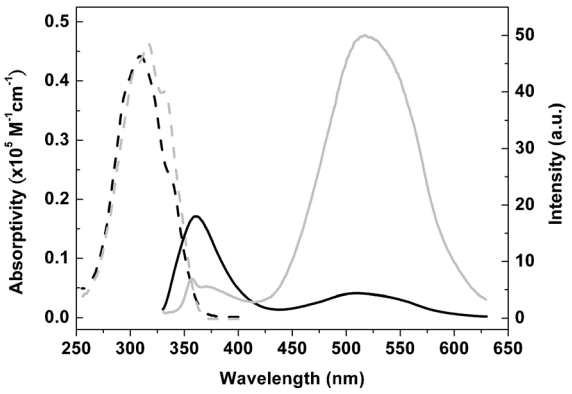

Figure 1. Absorption (-----) and emission (——) spectra of **2** (black) and **3** (gray) in THF (concentration $= 1 \times 10^{-5}$ M).

on the photophysical properties of the PET processes, **4** and **5** with ethylene and propylene bridges, respectively, were prepared. There was essentially no difference in their emission spectra (Figure 2). Based on these preliminary studies,

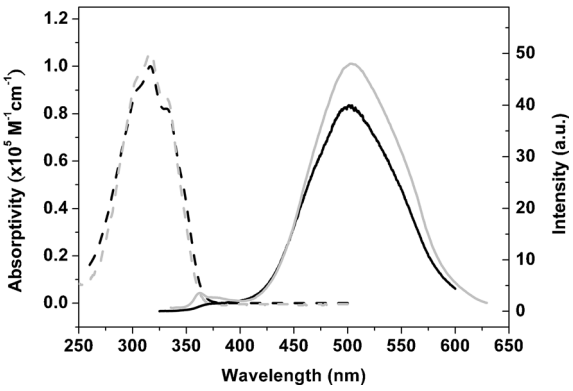

Figure 2. Absorption (-----) and emission (——) spectra of **4** (black) and **5** (gray) in THF (concentration $= 5 \times 10^{-6}$ M).

polymers **6** and **7** were designed and synthesized for the conformational investigations.

Synthesis: A rhodium(I)-catalyzed hydrosilylation protocol was used for the syntheses of **6** and **7** from the corresponding bis-alkyne **8** and bis-silyl hydride **9** or **10** shown in Equation (3).[14,22] The presence of one equivalent of NaI was essential to facilitate the rhodium-catalyzed hydrosilylation reactions.[18] Bis-alkyne **8** was obtained from the Sonogashira reaction of **11** and trimethylsilylacetylene followed by desilylation. Bis-silyl hydrides **9** and **10** containing acceptor chromophores were prepared from the metal/halogen exchange between bis-bromide **12** and *n*BuLi followed by reaction with R_2SiHCl, where R was a methyl or isopropyl group. The acceptor chromorphores in **9** and **10** were chosen so that the relative free-energy differences in the PET process for **6** could be tuned. In addition, the lengths of these acceptor chromophores were kept as close as possible to maintain similar center-to-center distances between the donor and acceptor chromophores in **6** and **7**.

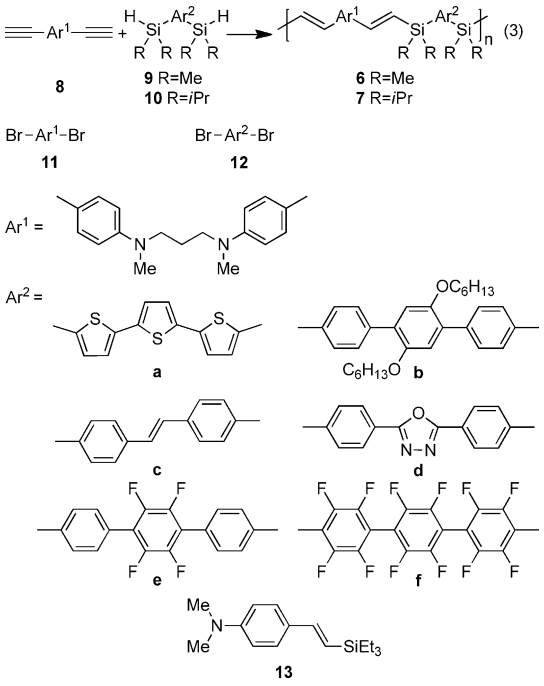

Photophysical and electrochemical properties of monomers 9 and 13: The photophysical properties, the redox potentials E_{ox} and E_{red}, and the relevant properties of monomers **9a–f** are compiled in Table 1. The frontier orbital energies for each of these chromophores were thus calculated. Accordingly, the PET would be expected from the HOMO of the aminostyrene moiety to the HOMO of the excited state of the chromophore in **9**.

Dissimilarity between $SiMe_2$- and Si*i*Pr_2-spaced copolymers based on steady-state spectroscopic analysis: As shown in Equation (3), a series of polymers **6** was designed so that the differences in the free energy ΔG_o for the charge separation processes were systematically tuned. By using the Weller equation,[23] the ΔG_o values in the electron-transfer process for **6** were estimated based on the data for the corresponding monomers **9** and **13** (Table 2).[22]

The absorption and emission spectra of **6**, **7**, and the corresponding acceptor monomers **9** in cyclohexane and THF are compared in Figures 3–9. Interestingly, the absorption spectra for **6** were essentially solvent independent. However, the absorption spectra for **7** exhibited noticeable additional absorption bands at longer wavelengths in cyclohexane and THF, which are attributed to the absorption for the charge-transfer complex.[24] Indeed, these lower-energy absorption bands shifted to further longer wavelengths with relatively higher intensities in the more-polar THF solvent than in cyclohexane. These results clearly indicate that interactions between the donor and acceptor chromophores at the ground state might be more significant in **7**, and thus the excitation pathways for **6** and **7** might be different.

The emission spectra of **6** and **7** exhibited completely different trends. The emission profile of **6a** in cyclohexane was almost identical to that of the corresponding monomer **9a** and the full-width half maxima (FWHM) of the emission band was only slightly broader in THF (Figure 3b). The emission intensities of **6a** in 2-methyltetrahydrofuran (MTHF) remained similar at diffferent temperatures in the range 298–180 K (Figure 3d). In the emission spectrum of **7a**, besides the LE emission of the acceptor chromophore at $\lambda = 424$ and 446 nm, a longer wavelength emission at approximately $\lambda = 450$–500 nm started to emerge (Figure 3c). Interestingly, the emission intensities of **7a** were enhanced with

Table 1. The photophysical and electrochemical properties of monomers **9** and **13**.

Compound	λ_{max}[a] [nm]	λ_{em}[a] [nm]	E_{0-0} [eV]	Φ[b]	τ_o[c] [ns]	E_{ox} [V]	E_{red} [V]	HOMO[d] [eV]	LUMO[e] [eV]
9a	365	424, 446	3.02	0.12	0.20	0.69	−2.48	−5.30	−2.67
9b	324, 273	396	3.41	0.80	1.00	0.89	−2.71	−5.50	−2.90
9c	320, 308	350, 366	3.62	0.26	0.18	1.24	−2.48	−5.85	−2.67
9d	292	345, 360	3.78	0.79	0.95	–	−2.37	–	−2.56
9e	265	344	4.05	0.28	1.95	–	−2.39	–	−2.58
9f	243	343	4.11	0.10	0.74	–	−2.18	–	−2.37
13	305	–	3.54	–	–	0.33	–	−4.94	−1.40

[a] The λ_{max} and λ_{em} values were measured in THF. [b] The Φ value was determined using coumarin-1 ($\Phi = 0.99$ in ethyl acetate) and 2,5-diphenyl-1,3,4-oxodiazole ($\Phi = 1.0$ in ethanol) as a standard. [c] Fluorescence lifetime τ_o was estimated by single-exponential fitting of the fluorescence decay profile. [d] HOMOs were estimated by oxidation potentials E_{ox} of **9a–c** and **13**. The E_{ox} values of **9d–f** were not measured because they were beyond the instrument limitation (1.3 V versus Ag/Ag^+). [e] LUMOs were estimated by reduction potential E_{red} of **9** and that of **13** was obtained by HOMO + E_{0-0}.

Table 2. Number-average molecular weight M_w, polydispersity index (PDI), and kinetic parameters of **6** and **7**.

	6				**7**		
	M_w (PDI)	$-\Delta G_o$[a] [eV]	τ_{CS}[b] [ps]	$k_{CS}\times10^{-10}$ [s^{-1}]	M_w (PDI)	τ_d [ps]	$k_d\times10^{-9}$ [s^{-1}]
a	17000 (1.6)	0.40	45	1.7	6500 (2.4)	38	12.0
						176	5.6
b	13000 (2.3)	0.56	34	2.9	7000 (1.6)	155	6.4
c	20000 (2.4)	1.01	9	10.6	6200 (2.0)	150	6.7
d	17800 (1.8)	1.27	14	7.0			
e	10600 (1.8)	1.52	19	5.2	5200 (1.7)	160	6.2
f	11800 (1.8)	1.79	35	2.7			

[a] Weller equation: $-\Delta G_o = E_{0-0} - e[E_{ox}(D) - E_{red}(A)] + C/R_{DA}$, where $C = e^2/4\pi\varepsilon_o\varepsilon_s = 3.04\times10^{-29}$ J m^{-1} and R_{DA} = center-to-center distance between the donor (D) and acceptor (A) chromophores in **6** estimated by the DFT calculations of model compounds **Ma**–**f**.[22] [b] Two-exponential fitting was utilized to give two lifetimes (see Figures S4–S6 in the Supporting Information),[22] in which the shorter component τ_{CS} was the major route for the fluorescence decay (~99%).

decreasing temperature (Figure 3e). The formation of the charge-transfer complex in **7a** might be plausible.

The dissimilarities in the emission properties between **6** and **7** were more prominent when $-\Delta G_o$ became larger. The emission spectrum of **6b** in cyclohexane at ambient temperature was the same as that of the corresponding monomeric acceptor chromophore **9b** (Figure 4b). It is worth noting that a shoulder appeared at approximately $\lambda = 480$ nm in THF. These dual fluorescence bands were assigned as the LE of the acceptor moiety at a shorter wavelength, and the CT emission at a longer wavelength.[25] When the two methyl substituents on the silicon atom in **6b** were replaced by two isopropyl groups, the emission spectrum of **7b** displayed a new emission profile at $\lambda = 420$–450 nm with a vibronic structure (Figure 4c). This emission behavior is consistent with the observation of a charge-transfer absorption band in **7b**, thus suggesting a strong intrachain interaction between the chromophores at the ground state. In the temperature-dependent emission spectra (Figure 4d,e), the emission intensities of **6b** were similar at different temperatures, whereas those of **7b** became stronger when the temperature was lowered. It is noteworthy that the variation in the emission intensities with temperature for **7b** appeared to be more prominent than those for **7a**.

When the $-\Delta G_o$ value was 1.01 eV, the emission spectrum of **6c** showed two emission bands at $\lambda = 360$ and 450 nm in cyclohexane due to LE and CT emissions, respectively (Figure 5b). When THF was employed, the relative LE intensity ($\lambda = 360$ nm) was significantly decreased. In addition, the relative intensity of the CT emission at approximately $\lambda =$ 530 nm became very prominent with a bathochromic shift in comparison with that observed in cyclohexane. On the other hand, the λ_{em} values for **7c** at $\lambda = 450$ and 480 nm in cyclohexane and THF, respectively (Figure 5c), were different from those observed for the LE and CT emissions for **6c**. The intensities of the CT emission in **6c** decreased significantly together with bathochromic shifts as the temperature was lowered (Figure 5d). Presumably, the solvent polarity may be enhanced as the temperature decreases,[26] and thus the charge-separation state might be stabilized to a lower energy level. It seems likely that the interaction between this excited state and the higher vibrational level of the ground state might result in a thermal-relaxation process to decrease the opportunity of radiative relaxation.[27,28] In contrast, the temperature-dependent behavior of emission profiles of **7c** was similar to that observed for **7b**, as described above (Figure 5e).

When the $-\Delta G_o$ value for the donor–acceptor couple was raised to 1.52 eV for **6e**, the emission profiles in cyclohexane and THF again became a single LE emission at $\lambda =$ 350 nm (Figure 6b) and were essentially temperature independent (Figure 6d). These properties were similar to those of **6a**, as described above. In other words, the emission spectra of **6a** and **6e** may have arisen mainly from the LE emission of the acceptor moiety and no emission at longer wavelengths arising from the CT emission being observed. On the other hand, the emission properties of **7e** in THF at ambient temperature and in MTHF at variable temperatures appeared to be similar to those of **7b** and **7c** (Figure 6c,e).

The presence of the geminal diisopropyl groups on the silicon atoms in **7** would exert the Thorpe–Ingold effect,[20] which may lead to modification of the average spacing and orientation between the donor and acceptor chromophores in **7** relative to those in **6**. Accordingly, the mode of the interactions between these donor and acceptor chromophores might lead to the discrepancy in photophysical behavior between these two series of copolymer. The absorption spectra of **6** were essentially the sum of all the contributing chromophores (in Figures 3–6), whereas those spectra of **7** consisted of an additional solvent-dependent absorption band at the longer wavelength because of the interactions between the donor and acceptor chromophores at the ground state; furthermore, the fluororescence observed for **7** might be attributed to the emission that arises from this charge-transfer complex.[25].

Steady-state observation of the Marcus-inverted region in 6: The $-\Delta G_o$ values for the charge-separation processes in the copolymers **6d** and **6f** were estimated to be 1.27 and 1.79 eV, respectively. The emission behaviors of **6d** (Figure 7a) and **6c** were comparable. However, the relative intensity of the LE versus CT emission for **6d** appeared to be more prominent than those for **6c** in both cyclohexane and THF solvents. It is worth mentioning that the ΔG_o value was

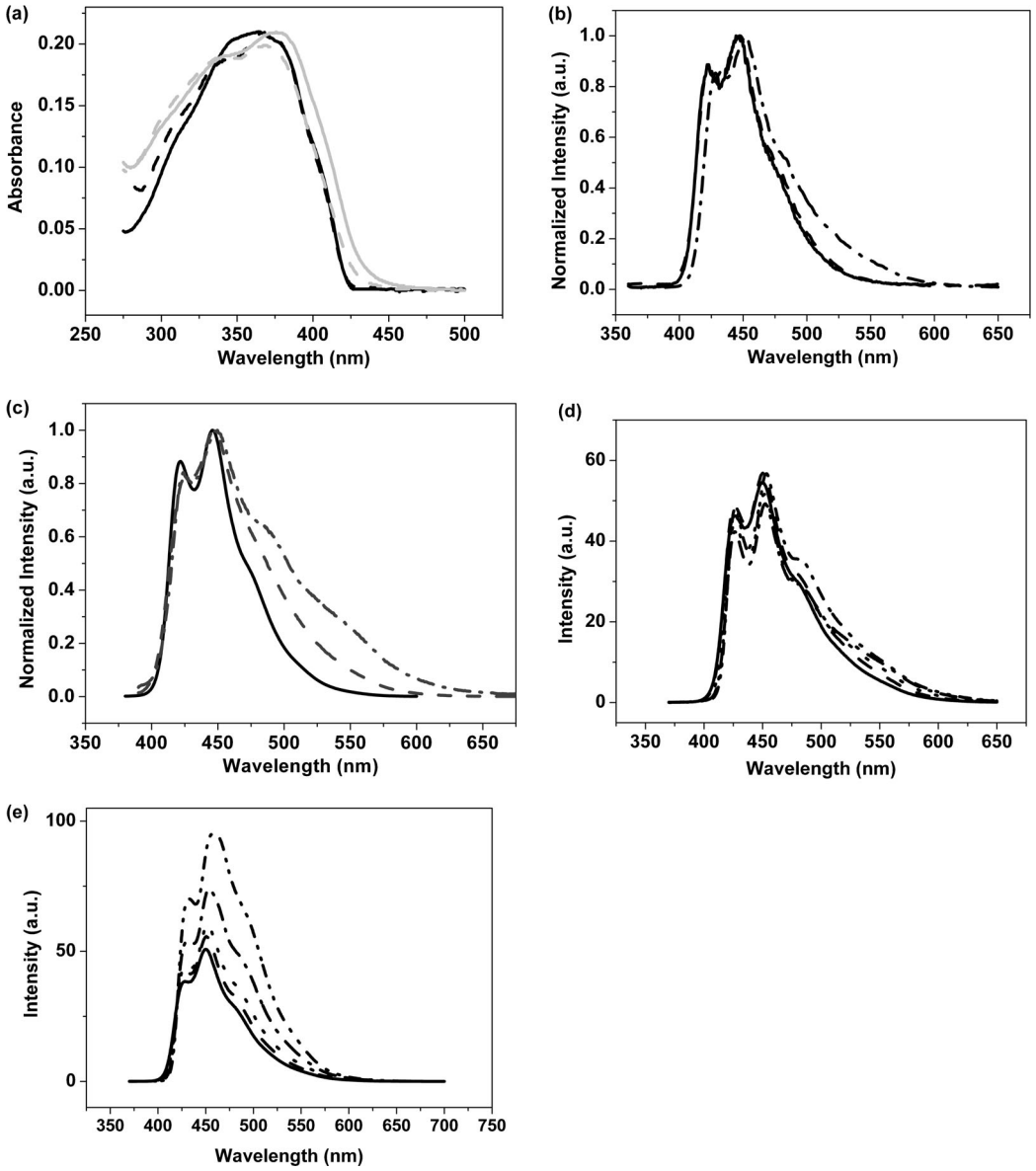

Figure 3. a) Absorption spectra of **6a** (black) and **7a** (gray) in cyclohexane (-----) and THF (——); concentration = 1.0×10^{-5} M. b) Emission spectra of **6a** in cyclohexane (-----) and THF (–•–•) and **9a** (——) in THF. c) Emission spectra of **7a** in cyclohexane (-----) and THF (–•–•) and **10a** (——) in THF. Variable-temperature emission spectra of d) **6a** and e) **7a** in MTHF (——: 298 K, -----: 270 K, •••••: 240 K, –•–•: 210 K, –••–••: 180 K; concentration = 1.0×10^{-5} M; excitation wavelength = 370 nm).

more negative for **6d** than for **6c**. As expected, the emission properties of **6f** (Figure 8a) were similar to those of **6e** because they represented relatively large $-\Delta G_o$ values. The temperature-dependent emission spectra of **6d** displayed a classic behavior of CT emission, as observed for **6c** (Figure 7b). Furthermore, **6f** behaved in a similar manner to **6e** when the temperature was changed (Figure 8b).

A plot of the integrated intensity ratios of CT (F_{CT}) and LE (F_{LE}) emissions for **6** against the $-\Delta G_o$ value is shown in Figure 9. It is interesting to note that the F_{CT}/F_{LE} ratios increased with increasing $-\Delta G_o$ value, reached a maximum, and then decreased again. These observations, based on the steady-state spectra, suggest that there was no CT emission when the $-\Delta G_o$ value was smaller than 0.5 eV or larger than 1.5 eV. The charge-transfer process became predominant when the $-\Delta G_o$ value was around 1 eV. These steady-state results matched nicely with the Marcus theory.[29] On the contrary, no similar behavior was found with copolymer **7**.

Time-resolved fluorescence spectroscopy: Time-resolved fluorescence spectroscopy with a femtosecond Ti/sapphire laser and a streak camera was employed to obtain the emission decays of **6** and **7** (see Figures S1–S3 in the Supporting Information). The LE emission wavelengths of the corresponding acceptor chromophores in **6** were monitored, and the decay lifetimes attributed to charge-separation process

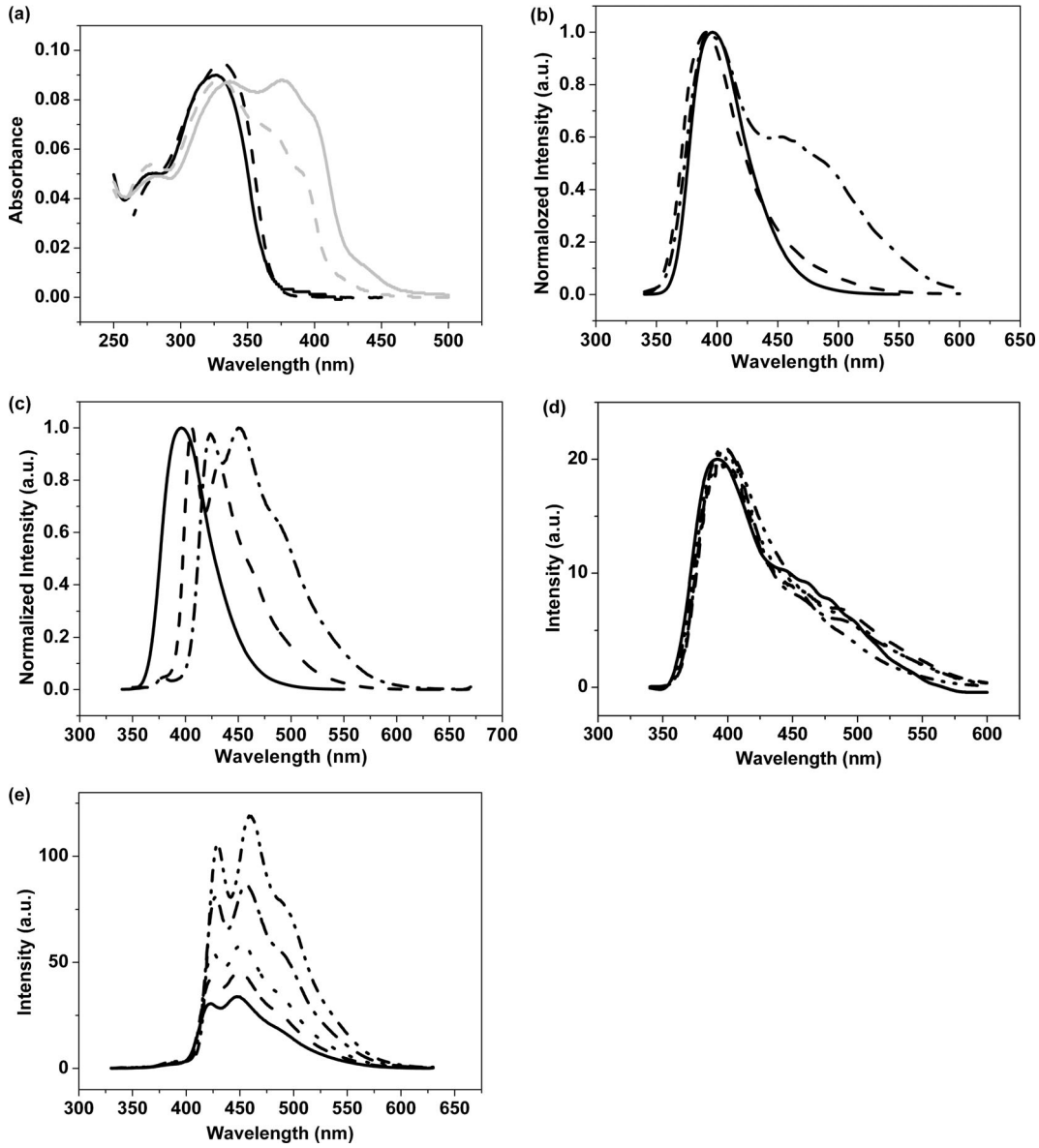

Figure 4. a) Absorption spectra of **6b** (black) and **7b** (gray) in cyclohexane (-----) and THF (——); concentration = 1.0×10^{-5} M. b) Emission spectra of **6b** in cyclohexane (-----) and THF (–•–•) and **9b** (——) in THF. c) Emission spectra of **7b** in cyclohexane (-----) and THF (–•–•) and **10b** (——) in THF. Variable-temperature emission spectra of d) **6b** and e) **7b** in MTHF (——: 298 K, -----: 270 K, •••••: 240 K, –•–•: 210 K, –••–••: 180 K; concentration = 1.0×10^{-5} M; excitation wavelength = 370 nm).

were obtained (Table 2). The rate constants of charge separation processes k_{CS} were thus calculated.[30] When the ΔG_o values became more negative, the k_{CS} values increased initially, reached a maximum, and then decreased. A plot of k_{CS} against $-\Delta G_o$ is shown in Figure 10. Notably, the Marcus-inverted region was observed for the first time based on forward PET processes in a polymeric system.

Polymers **6c** and **6d** exhibited dual emissions, from which the CT emissions at longer wavelengths were prominent (in Figure 5b and 7a). The fluorescence decay at these wavelengths as a result of the CT emission were monitored, and these lifetimes were 4.5 and 2.6 ns for **6c** and **6d**, respectively. The corresponding rate constant of the charge-recombination process was calculated to be $k_{CR}=2.2$ and $3.8\times10^8\ s^{-1}$. The free-energy changes of these relaxation processes of **6c** and **6d** (determined by $-\Delta G_{CR}=E_{0-0}+\Delta G_o$) were $-\Delta G_{CR}=2.63$ and 2.52 eV, respectively. It is worth mentioning that these k_{CR} values fitted nicely into the inverted region. The emission lifetimes τ_d for **7** and the rate of the deactivation processes k_d are also listed in Table 2. It is interesting to note that the emission-decay profile of **7a** was treated by a two-exponential fitting to give two lifetimes $\tau_d=38$ and 176 ps. The magnitude of the longer lifetime was similar to other τ_d values of **7b**, **7c**, and **7e**, and the magnitude of the shorter lifetime was close to τ_{CS} values of **6a**. These results were consistent with the steady-emission spec-

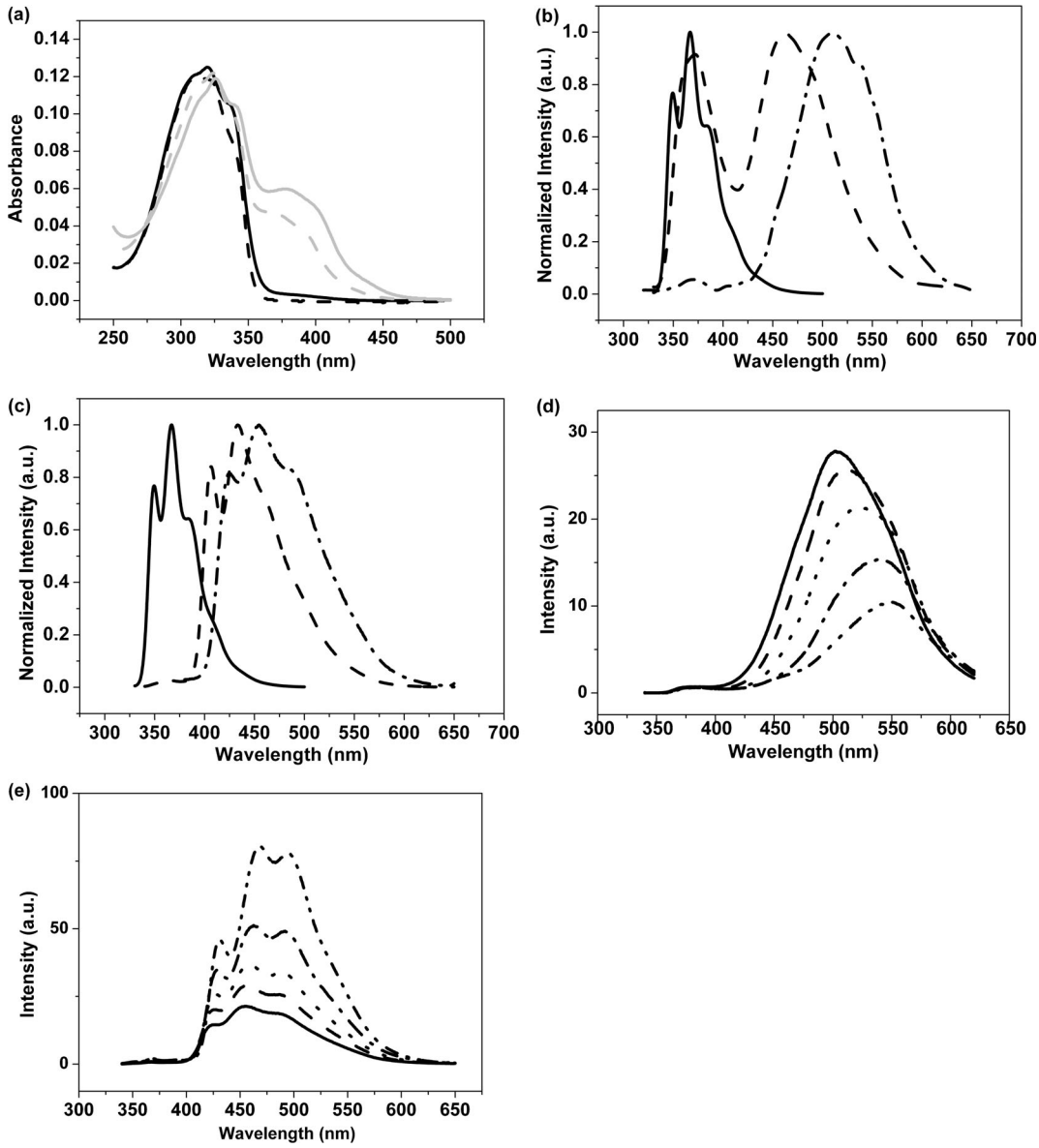

Figure 5. a) Absorption spectra of **6c** (black) and **7c** (gray) in cyclohexane (-----) and THF (——); concentration = 1.0×10^{-5} M. b) Emission spectra of **6c** in cyclohexane (-----) and THF (–•–•) and **9c** (——) in THF. c) Emission spectra of **7c** in cyclohexane (-----) and THF (–•–•) and **10c** (——) in THF. Variable-temperature emission spectra of d) **6c** and e) **7c** in MTHF (——: 298 K, -----: 270 K, •••••: 240 K, –•–•: 210 K, –••–••: 180 K; concentration = 1.0×10^{-5} M; excitation wavelength = 330 nm).

tra of **7a**, in which the emission spectra showed a broad band that possibly involved two different radiative-relaxation processes from the LE emission of the acceptor and the emission of the charge-transfer complex. The k_d values for **7** were similar, whereas the k_{CS} and k_{CR} values for **6** followed a bell-shape distribution (Table 2).

It seems likely that the electronic coupling between the LE and CT states in **6** and **7** would be different, thus leading to different radiative-relaxation pathways. These results reiterate the discrepancy of the alkyl substituents on the silicon atom on the conformations of **6** and **7** due to the Thorpe–Ingold effect, which would dictate the photophysical behavior of the donor–acceptor pair in these copolymers. Indeed, a broad transient maximum at $\lambda = 530$ nm was characterized in **6c**, but there was no transient feature at $\lambda = 530$ nm in **7c** (Figure 11). These results further confirmed that the transient species of the excited state were different for **6c** and **7c**.

Thorpe–Ingold effect and polymer folding: It is known that silylene-spaced divinylarene and related copolymers are highly folded.[13,14] Through-space interactions between nonadjacent divinylbenzene chromophores readily take place to result in the appearance of emission bands at longer wavelengths with vibronic fine structures.[15] To rule out such a possibility, copolymers **14a** and **14b** were synthesized by replacing the *N*-methyl amino groups in **6** and **7** with ethyli-

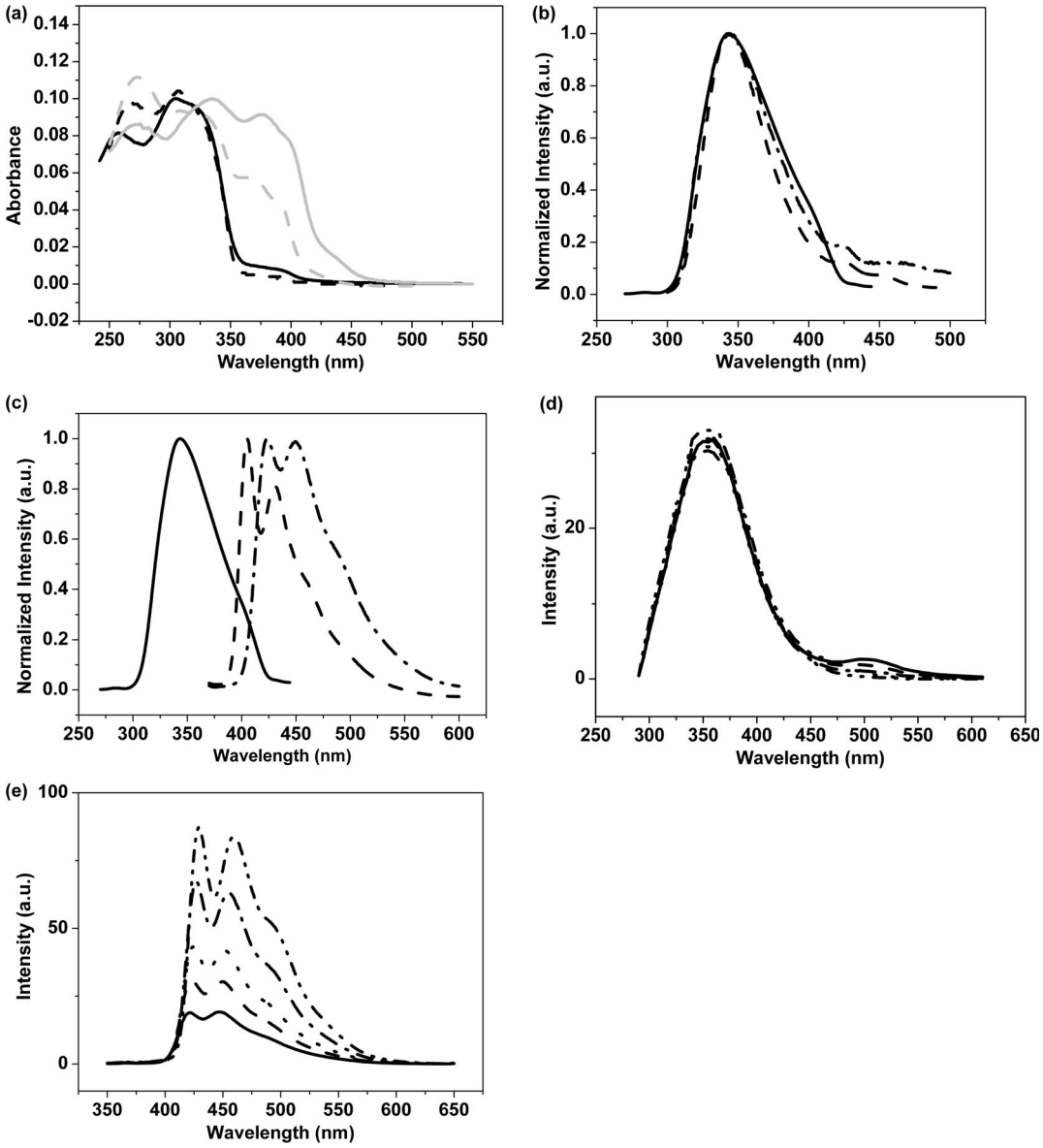

Figure 6. a) Absorption spectra of **6e** (black) and **7e** (gray) in cyclohexane (-----) and THF (——); concentration = 1.0×10^{-5} M. b) Emission spectra of **6e** in cyclohexane (-----) and THF (–•–•), and **9e** (——) in THF. c) Emission spectra of **7e** in cyclohexane (-----) and THF (–•–•), and **10e** (——) in THF. Variable-temperature emission spectra of d) **6a** and e) **7e** in MTHF (——: 298 K, -----: 270 K, •••••: 240 K, –•–•: 210 K, –••••–: 180 K; concentration = 1.0×10^{-5} M; excitation wavelength = 290 nm).

dene moieties. No PET process between the stilbene chromophore and *para*-alkyl-substituted styrene moieties would be expected as a result of the mismatch of the frontier orbital energies. The absorption and emission spectra of **14a** and **14b** are shown in Figure 12. Similar fluorescence spectra of

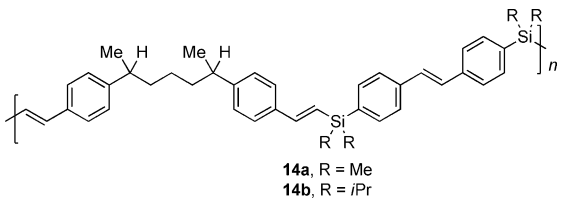

14a, R = Me
14b, R = *i*Pr

14a and **14b** as a result of the intrinsic emission of the stilbene chromophore suggest that no intrachain through-space interactions that lead to the longer-wavelength emissions in these polymers would take place, no matter whether the substituent on the silicon atom is a methyl or isopropyl group. These results indicate the absorption and emission features observed in **7** would arise from the charge-transfer complex.

The experimental evidence discussed above suggests the importance of the Thorpe–Ingold effect on the conformation of the dialkylsilylene-spaced copolymers **6** and **7**, which would bring the adjacent donor–acceptor chromophores in proximity. As such, the mode of interaction between these

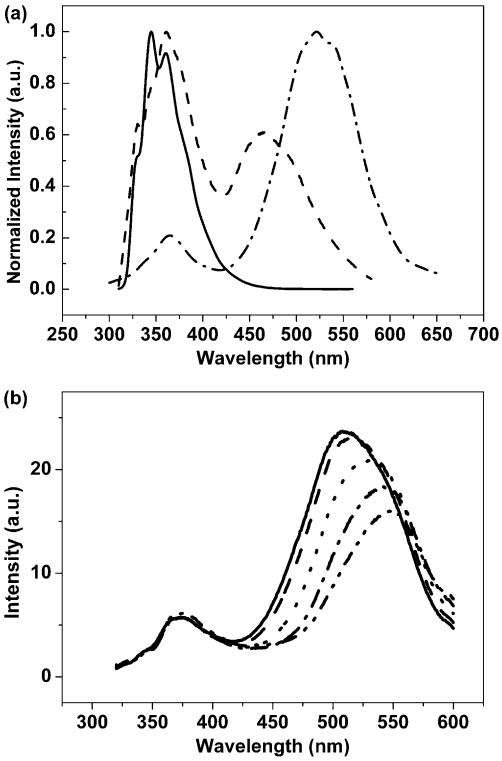

Figure 7. a) Emission spectra of **9d** (——) in THF and **6d** in cyclohexane (-----) and THF (–•–•). b) Variable-temperature emission spectra of **6d** in MTHF (——: 298 K, -----: 270 K, •••••: 240 K, –•–•: 210 K, –••–••: 180 K; concentration = 1.0×10^{-5} M; excitation wavelength = 290 nm).

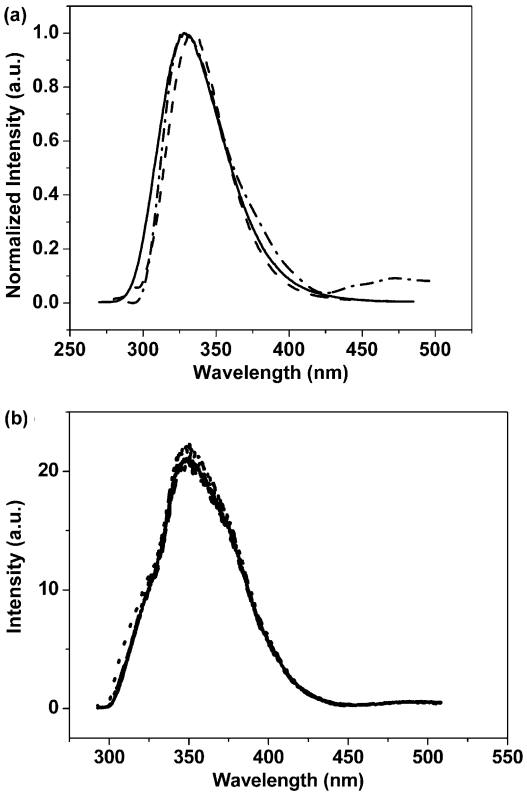

Figure 8. a) Emission spectra of **9f** (——) in THF and **6f** in cyclohexane (-----) and THF (–•–•). b) Variable-temperature emission spectra of **6f** in MTHF (——: 298 K, -----: 270 K, •••••: 240 K, –•–•: 210 K, –••–••: 180 K; concentration = 1.0×10^{-5} M; excitation wavelength = 280 nm).

chromophores would be different depending on the steric bulkiness of the substituents on the silicon atom. For the purpose of establishing the importance of the interactions between adjacent donor–acceptor chromophores modulated by silylene moieties in **6** and **7**, the monomeric model donor–acceptor pairs **2** and **15** were synthesized. The ab-

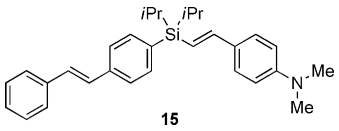

15

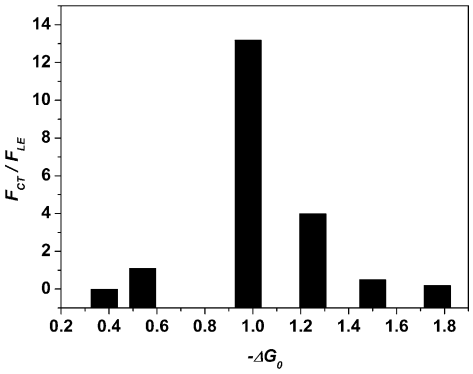

Figure 9. The relative ratios of CT/LE emission intensity of **6a–f** in THF.

sorption spectra were essentially independent of the solvent polarity (see Figure S7 in the Supporting Information), and there is no characteristic charge-transfer absorption for **2** and **15**. The emission spectra of **2** and **15** are compared with those of **6c** and **7c** in Figure 13a,b, respectively. The emission spectrum of **2** in cyclohexane showed LE emission of the acceptor moiety at $\lambda = 370$ nm and a tailing signal toward $\lambda = 450$ nm. When THF was used as the solvent, dual emissions were observed at $\lambda = 370$ and 510 nm, and these two emissions were assigned to LE and CT emissions, respectively, which is similar to those of **6c**. The emission spectrum of **15** also displayed the LE and CT emissions at $\lambda = 370$ and 450 nm, respectively, in cyclohexane; furthermore, the CT emission shifted to $\lambda = 510$ nm in THF. Interestingly, the emission profiles of **15** were similar to those of **2** or **6c**, but completely different from those of **7c** under the same conditions. Unlike the emissions of **7c**, no emission as a result of the charge-transfer complex was observed at all for **15**, although both **7c** and **15** contain the $i\mathrm{Pr}_2\mathrm{Si}$ linker between the donor and acceptor chromophores. As discussed above, the bulky isopropyl substituents would exert the Thorpe–Ingold effect to bring the adjacent chromophores into proximity. Compound **15** is a small molecule. Rotation about the sigma bonds might occur relatively freely, thus

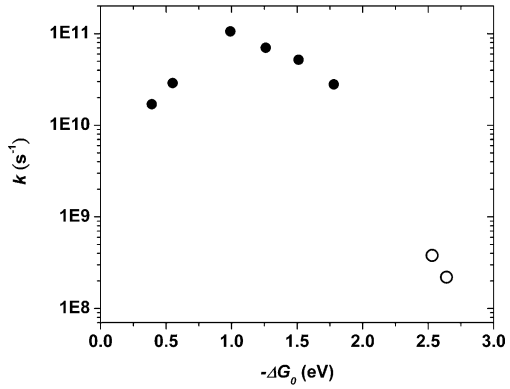

Figure 10. Logarithmic plots of rate constants versus free-energy change of the forward (●) and backward (○) electron-transfer reactions.

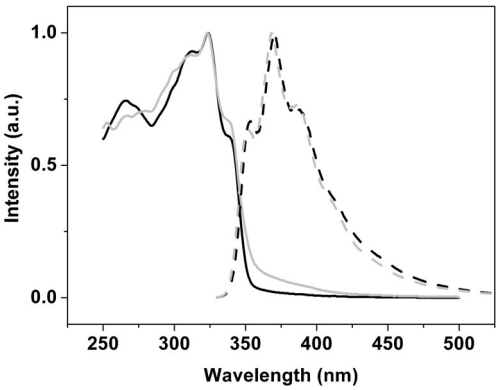

Figure 12. The normalized absorption (——) and emission (-----) spectra of **14a** (black) and **14b** (gray) measured in THF.

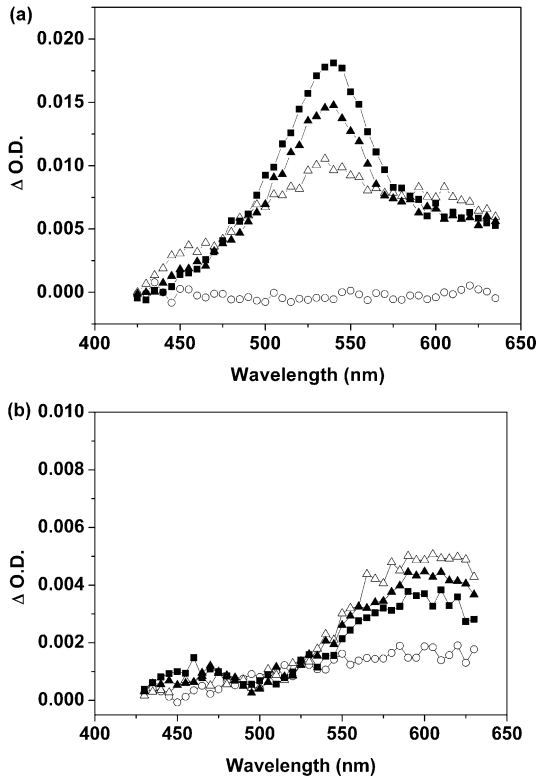

Figure 11. Transient absorption spectra of a) **6c** and b) **7c** (○: 0 ps, △: 1 ps, ▲: 3 ps, ■: 10 ps).

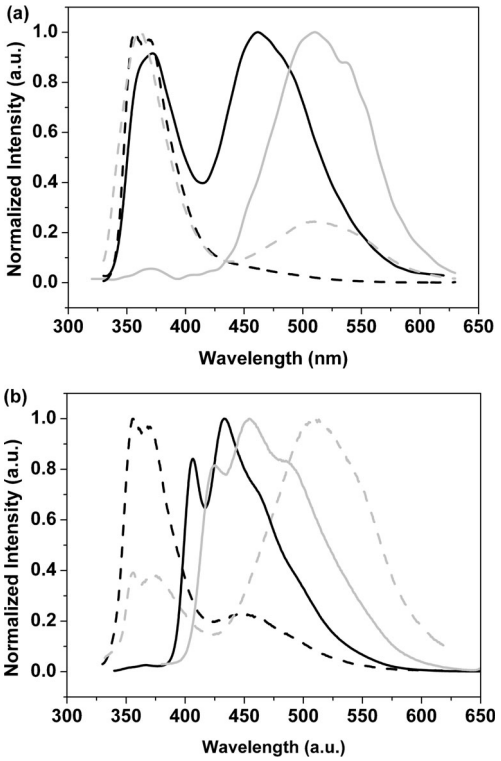

Figure 13. The emission spectra of a) **2** (-----) and **6c** (——) and b) **15** (-----) and **7c** (——) in cyclohexane (black) and THF (gray). Excitation wavelength = 330 nm.

leading to an ensemble of different conformers. The distance between the donor and acceptor chromophores might not be fixed in **15**. Accordingly, the mode of interaction between the donor and acceptor chromophores for **2** and **15** would be similar. It is worth noting that the relative intensity of the CT emission of **15** was much stronger than that of **2**. Presumably, the Thorpe–Ingold effect remained to play an important role. On the other hand, silylene-spaced copolymers would be highly folded and the Thorpe–Ingold effect may generate a variation in the local conformation. Such a change in the local conformation may lead to a different folding nature of a polymer. It seems likely that the folding of polymer **7c** might further perturb the relative distance between the adjacent donor and acceptor chromophores, thus resulting in different photophysical behavior.

Random copolymers **16** with different ratios of Me_2Si and iPr_2Si linkers ($Me_2Si/iPr_2Si = 9:1$, 4:1, and 1:1) were synthesized. The absorbance of the charge-transfer absorption at approximately $\lambda = 400$ nm increases with increasing molar fractions of the iPr_2Si moieties (Figure 14a). The relative intensity of the emission at $\lambda = 510$ nm (Figure 14b), as a result of the CT emission from the donor–acceptor pair linked by the Me_2Si spacer, decreases with decreasing molar

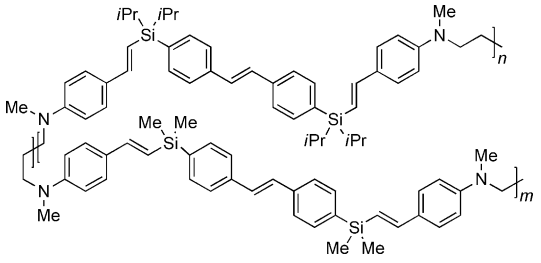

16

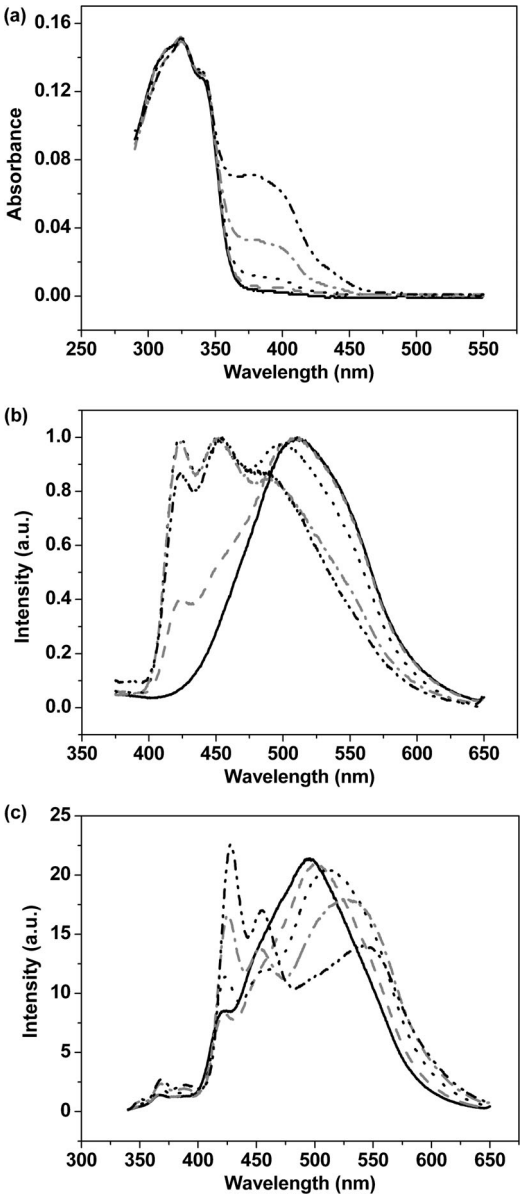

Figure 14. a) Absorption and b) emission spectra of **6c**, **7c**, and **16** with different ratios of Me_2Si and iPr_2Si spacers (——: **6c**, -----: **16** $Me_2Si/iPr_2Si = 9:1$, •••••: **16** $Me_2Si/iPr_2Si = 4:1$, –•–•: **16** $Me_2Si/iPr_2Si = 1:1$, –••–••: **7c**; concentration $= 4.5 \times 10^{-6}$ M). c) Variable-temperature emission spectra of **16** ($SiMe_2/SiiPr_2 = 9:1$) in MTHF (——: 298 K, -----: 270 K, •••••: 240 K, –•–•: 210 K, –••–••: 180 K; concentration $= 1.0 \times 10^{-5}$ M; excitation wavelength = 330 nm).

fraction of the Me_2Si linkers in **16**. In the meantime, the emission at $\lambda = 450$ nm, which arises from the emission from the iPr_2Si-spaced donor–acceptor pair, became stronger when the molar fraction of the iPr_2Si spacer increases. As expected, the intensity of the emission band at approximately $\lambda = 450$ nm increases with decreasing temperature, whereas that of the emission band at around $\lambda = 500$–550 nm decreases with concomitant bathchromic shift at the same time. These behaviors are same as the temperature-dependent emissions of **6c** and **7c** discussed previously. In other words, when the donor and acceptor chromophores were spaced by the iPr_2Si group, a charge-transfer complex would be formed between these chromophores in the polymers and the emission of the Me_2Si-spaced donor–acceptor pair in **16** exhibits typical CT emissions as those observed for **6c**. These results suggest that concomitance of the Thorpe–Ingold effect and polymer folding is indispensable to control the electronic interactions between adjacent donor–acceptor chromophores.

Conclusion

In summary, we have demonstrated the fundamental differences between the photophysical properties of **6** and **7** owing to a difference in the alkyl substituents on the silylene spacer. The variation of the steric environment around the silicon atom may generate different conformations and folding so that the spatial arrangement and orientation of the donor and acceptor chromophores could be adjusted. The free-energy differences between the LE and CT states for **6** could readily be tuned and dual emissions were observed in those polymers with appropriate the ΔG_o values for the charge-separation processes. In particular, the Marcus-inverted region was observed in both steady-state and fast kinetic measurements for **6**. In contrast, the photophysical behavior is completely different when the substituents on the silicon atom are changed from dimethyl to diisopropyl groups. Because of the synchronized Thorpe–Ingold effect exerted by the bulky isopropyl substituents and the perturbation of the conformation of the polymer, the adjacent donor and acceptor chromophores in **7** may be brought closer. A charge-transfer complex may thus be formed from a strong interaction between these neighboring chromophores at the ground state. Evidence to support the importance of folding on the photophysical behavior of **6** and **7** can be illustrated by a systematic investigation on the oligomers with the same structural features of **6** and **7**.[31]

Experimental Section

General: Gel-permeation chromatography (GPC) was performed on a Waters GPC machine with an isocratic HPLC pump (1515) and a refractive-index detector (2414). THF was used as the eluent (flow rate = 1.0 mL min^{-1}). Waters Styragel HR2, HR3, and HR4 columns (7.8 × 300 mm) were employed for determination of the relative molecular weight with polystyrene as a standard (M_n values ranged from 375 to

3.5×10^6). Absorption spectra were measured on a Hitachi U-3310 spectrophotometer and emission spectra on a Hitachi F-4500 fluorescence spectrophotometer. An ECO Chemie μAutolab III potentiostat/galvanostat was used for the electrochemical experiments in which Pt electrodes were used as the working and counter electrodes and a $Ag/AgNO_3$ electrode was used as the reference electrode.

Time-resolved fluorescence experiments: A mode-locked Ti/sapphire laser (repetition rate: 76 MHz; pulse width: <200 fs) passed through an optical parametric amplifier to produce the desired wavelength of the pulse laser. The fluorescence of the sample was reflected by a grating (150 g mm^{-1}; BLZ: 500 nm) and detected by an optically triggered streak camera (Hamamatsu C5680) with a time resolution of about 0.3 ps. The sample was prepared in a concentration of 1.0×10^{-5} M, and using an ultramicro cuvette with a pathlength of 1 mm to maintain the excitation at the same time. The signal was collected ten times to decrease the signal-to-noise ratio.

Acknowledgements

This work was supported by the National Science Council and the National Taiwan University of the Republic of China. We thank Professors Yuan-Chung Cheng, Bih-Yaw Jin, and Chao-Ping Hsu for helpful discussions and Professor Huan-Cheng Chang for allowing us to use the femtosecond laser facilities for kinetic measurements.

[1] S. Hecht, I. Huc, *Foldamers*, Wiley-VCH, Weinheim, **2007**.

[2] For reviews, see: a) L. Brunsveld, B. J. B. Folmer, E. W. Meijer, R. P. Sijbesma, *Chem. Rev.* **2001**, *101*, 4071–4097; b) D. J. Hill, M. J. Mio, R. B. Prince, T. S. Hughes, J. S. Moore, *Chem. Rev.* **2001**, *101*, 3893–4011.

[3] a) M. Fathalla, C. M. Lawrence, N. Zhang, J. L. Sessler, J. Jayawickramarajah, *Chem. Soc. Rev.* **2009**, *38*, 1608–1620; b) J. L. Sessler, J. Jayawickramarajah, *Chem. Commun.* **2005**, 1939–1949; c) S. Yagai, *J. Photochem. Photobiol. C* **2006**, *7*, 164–182; d) J. R. Rudick, V. Percec, *Acc. Chem. Res.* **2008**, *41*, 1641–1652; e) E. Yashima, K. Maeda, H. Lida, Y. Furusho, K. Nagai, *Chem. Rev.* **2009**, *109*, 6102–6211.

[4] a) M. Hagihara, N. J. Anthony, T. J. Stout, J. Clardy, S. L. Schreiber, *J. Am. Chem. Soc.* **1992**, *114*, 6568–6570; b) J. H. K. K. Hirschberg, L. Brunsveld, A. Ramzi, J. A. J. M. Vekemans, R. P. Sijbesma, E. W. Meijer, *Nature* **2000**, *407*, 167–170; c) P. Cordier, F. Tournilhac, C. Soulié-Ziakovic, L. Leibler, *Nature* **2008**, *451*, 977–980; d) E. J. Foster, E. B. Berda, E. W. Meijer, *J. Am. Chem. Soc.* **2009**, *131*, 6964–6966.

[5] a) V. N. Uversky, E. A. Permyakov, *Method in Protein Structure and Stability Analysis*, Nova Biomedical, New York, **2007**; b) A. Tramontano, *Protein Structure Prediction: Concepts and Applications*, Wiley-VCH, Weinheim, **2006**; c) J. Buchner, Y. Kiefhaber, *Protein Folding Handbook*, Wiley-VCH, Weinheim, **2005**.

[6] For reviews, see: a) R. P. Cheng, S. H. Gellman, W. F. Degrado, *Chem. Rev.* **2001**, *101*, 3219–3232; b) G. D. Rose, P. J. Fleming, J. R. Banavar, A. Maritan, *Proc. Natl. Acad. Sci. USA* **2006**, *103*, 16623–16633; c) A. Patgiri, A. L. Jochin, P. S. Arora, *Acc. Chem. Res.* **2008**, *41*, 1289–1300.

[7] For reviews, see: a) E. A. Meyer, R. K. Castellano, F. Diederich, *Angew. Chem.* **2003**, *115*, 1244–1287; *Angew. Chem. Int. Ed.* **2003**, *42*, 1210–1250; b) D. Pijper, B. L. Feringa, *Soft Matter* **2008**, *4*, 1349–1372; c) A. Berresheim, M. Müller, K. Müllen, *Chem. Rev.* **1999**, *99*, 1747–1785; d) P. Leclère, E. Hennebicq, A. Calderone, P. Brocorens, A. C. Grimsdale, K. Müllen, J. L. Brédas, R. Lazzaroni, *Prog. Polym. Sci.* **2003**, *28*, 55–81; e) F. J. M. Hoeben, P. Jonkheijm, E. W. Meijer, A. P. H. J. Schennung, *Chem. Rev.* **2005**, *105*, 1491–1546.

[8] For a review, see: J. W. Lockman, N. M. Paul, J. R. Parquette, *Prog. Polym. Sci.* **2005**, *30*, 423–452.

[9] a) K. Kirshenbaum, A. E. Barron, R. A. Goldsmith, P. Armand, E. K. Bradley, K. T. V. Truong, K. A. Dill, F. E. Cohen, R. N. Zuckermann, *Proc. Natl. Acad. Sci. USA* **1998**, *95*, 4303–4308; b) E. Yashima, T. Matsushima, Y. Okamoto, *J. Am. Chem. Soc.* **1997**, *119*, 6345–6359; c) R. Nonokawa, E. Yashima, *J. Am. Chem. Soc.* **2003**, *125*, 1278–1283; d) R. B. Prince, L. Brunsveld, E. W. Meijer, J. S. Moore, *Angew. Chem.* **2000**, *112*, 234–236; *Angew. Chem. Int. Ed.* **2000**, *39*, 228–230.

[10] a) R. B. Prince, J. G. Saven, P. G. Wolynes, J. S. Moore, *J. Am. Chem. Soc.* **1999**, *121*, 3114–3121; b) J. Kim, T. M. Swager, *Nature* **2001**, *411*, 1030–1034; c) J. Kim, I. A. Levitsky, D. T. McQuade, T. M. Swager, *J. Am. Chem. Soc.* **2002**, *124*, 7710–7718.

[11] For reviews see: a) M. R. Wasielewski, *Chem. Rev.* **1992**, *92*, 435–461; b) Z. R. Grabowski, K. Rotkiewicz, *Chem. Rev.* **2003**, *103*, 3899–4031; c) S. Doose, H. Neuweiler, M. Sauer, *ChemPhysChem* **2009**, *10*, 1389–1398.

[12] a) V. Balzani, *Electron Transfer in Chemistry, Vol. 1*, Wiley, New York, **2001**; b) V. May, O. Kühn, *Charge and Energy Transfer Dynamics in Molecular Systems*, Wiley-VCH, Weinheim, **2004**.

[13] For reviews, see: a) J. R. Winkler, H. B. Gray, *Chem. Rev.* **1992**, *92*, 369–379; b) N. Mataga, H. Chosrowjan, S. Taniguchi, *J. Photochem. Photobiol. C* **2004**, *5*, 155–168; c) X. Michalet, S. Weiss, M. Jäger, *Chem. Rev.* **2006**, *106*, 1785–1813; d) M. Y. Berezin, S. Achilefu, *Chem. Rev.* **2010**, *110*, 2641–2684.

[14] For reviews see: T.-Y. Luh, Y.-J. Cheng, *Chem. Commun.* **2006**, 4669–4678.

[15] a) R.-M. Chen, K.-M. Chien, K.-T. Wong, B.-Y. Jin, T.-Y. Luh, J.-H. Hsu, W. Fann, *J. Am. Chem. Soc.* **1997**, *119*, 11321–11322; b) Y.-J. Cheng, S. Basu, S.-j. Luo, T.-Y. Luh, *Macromolecules* **2005**, *38*, 1442–1446; c) M.-Y. Yeh, H.-C. Lin, S.-L Lee, C.-h. Chen, T.-S. Lim, W. Fann, T.-Y. Luh, *Chem. Commun.* **2007**, 3459–3461.

[16] a) Y.-J. Cheng, T.-Y. Hwu, J.-H. Hsu, T.-Y. Luh, *Chem. Commun.* **2002**, 1978–1979; b) Y.-J. Cheng, T.-Y. Luh, *Chem. Eur. J.* **2004**, *10*, 5361–5368; c) Y.-J. Cheng, T.-Y. Luh, *Macromolecules* **2005**, *38*, 4563–4568; d) K.-L. Liu, S.-J. Lee, I.-C. Chen, C.-P. Hsu, M.-Y. Yeh, T.-Y. Luh, *J. Phys. Chem. A* **2009**, *113*, 1218–1224.

[17] a) Y.-J. Cheng, H. Liang, T.-Y. Luh, *Macromolecules* **2003**, *36*, 5912–5914; b) M.-Y. Yeh, T.-Y. Luh, *Chem. Asian J.* **2008**, *3*, 1620–1624.

[18] a) H.-W. Wang, Y.-J. Cheng, C.-H. Chen, T.-S. Lim, W. Fann, C.-L. Lin, Y.-P. Chang, K.-C. Lin, T.-Y. Luh, *Macromolecules* **2007**, *40*, 2666–2671; b) M.-Y. Yeh, H-C. Lin, S.-L. Lee, C.-h. Chen, T.-S. Lim, W. Fann, T.-Y. Luh, *Macromolecules* **2007**, *40*, 9238–9243; c) H.-W. Wang, M.-Y. Yeh, C.-H. Chen, T.-S. Lim, W. Fann, T.-Y. Luh, *Macromolecules* **2008**, *41*, 2762–2770; d) C. A. van Walree, M. R. Roest, W. Schuddeboom, L. W. Jenneskens, J. W. Verhoeven, J. M. Warman, H. Kooijman, A. L. Spek, *J. Am. Chem. Soc.* **1996**, *118*, 8395–8407; e) A. Zehnacker, F. Lahmani, C. A. van Walree, L. W. Jenneskens, *J. Phys. Chem. A* **2000**, *104*, 1377–1387.

[19] a) J. Ohshita, D. Kanaya, M. Ishikawa, T. Koike, T. Yamanaka, *Macromolecules* **1991**, *24*, 2106–2107; b) A. Kunai, E. Toyoda, I. Nagamoto, T. Horio, M. Ishikawa, *Organometallics* **1996**, *15*, 75–83; c) M.-C. Fang, A. Watanabe, M. Matsuda, *Macromolecules* **1996**, *29*, 6807–6813; d) R. Gleiter, W. Schäfer, H. Sakurai, *J. Am. Chem. Soc.* **1985**, *107*, 3046–3050; e) W.-Y. Wong, C.-K. Wong, G.-L. Lu, A. W.-M. Lee, K.-W. Cheah, J. X. Shi, *Macromolecules* **2003**, *36*, 983–990.

[20] T.-Y. Luh, Z. Hu, *Dalton Trans.* **2010**, *39*, 9185–9192.

[21] a) F. D. Lewis, D. M. Bassani, E. L. Burch, B. E. Cohen, J. A. Engleman, G. D. Reddy, S. Schneider, W. Jaeger, P. Gedeck, M. Gahr, *J. Am. Chem. Soc.* **1995**, *117*, 660–669; b) J. Herbich, A. Kapturkiewicz, *J. Am. Chem. Soc.* **1998**, *120*, 1014–1029; c) U. Pischel, X. Zhang, B. Hellrung, E. Haselbach, P.-A. Muller, W. M. Nau, *J. Am. Chem. Soc.* **2000**, *122*, 2027–2034.

[22] The details are given in the Supporting Information.

[23] a) D. Rehm, A. Weller, *Isr. J. Chem.* **1970**, *8*, 259–271; b) A. Weller, *Z. Phys. Chem. (Muenchen Ger.)* **1982**, *133*, 93–98.

[24] R. S. Mulliken, W. B. Person, *Molecular Complexes*, Wiley, New York, **1969**.

[25] P. Pasman, G. F. Mes, N. W. Koper, J. W. Verhoeven, *J. Am. Chem. Soc.* **1985**, *107*, 5839–5843.
[26] J. A. Riddick, W. B. Bunger, T. K. Sakano, *Organic Solvent, Physical Properties and Methods of Purification*, Wiley, New York, **1986**.
[27] a) J. V. Caspar, T. J. Meyer, *J. Phys. Chem.* **1983**, *87*, 952–957; b) J. Kurzawa, S. Scheider, J. Büber, R. Gleiter, T. Clark, *Phys. Chem. Chem. Phys.* **2004**, *6*, 3811–3823; c) M. Tachiya, K. Seki, *J. Phys. Chem. A* **2007**, *111*, 9553–9559.
[28] For a review, see: N. Mataga, H. Chrosrowjan, S. Taniguchi, *J. Photochem. Photobiol. C* **2005**, *6*, 37–79.
[29] a) R. A. Marcus, *J. Chem. Phys.* **1956**, *24*, 966–978; b) J. R. Miller, L. T. Calcaterra, G. L. Closs, *J. Am. Chem. Soc.* **1984**, *106*, 3047–3049; c) G. L. Closs, J. R. Miller, *Science* **1988**, *240*, 440–447; d) M. R. Wasielewski, M. P. Niemczyk, W. A. Svec, E. B. Pewitt, *J. Am. Chem. Soc.* **1985**, *107*, 1080–1082; e) P. Chen, R. Duesing, G. Tapolsky, T. J. Meyer, *J. Am. Chem. Soc.* **1989**, *111*, 8305–8306; f) C. Zou, J. B. Miers, R. M. Ballew, D. D. Dlott, G. B. Schuster, *J. Am. Chem. Soc.* **1991**, *113*, 7823–7825; g) E. H. Yonemoto, R. L. Riley, Y. I. Kim, S. J. Atherton, R. H. Schmehl, T. E. Mallouk, *J. Am. Chem. Soc.* **1992**, *114*, 8081–8087; h) A. N. Macpherson, P. A. Liddell, S. Lin, L. Noss, G. R. Seely, J. M. DeGraziano, A. L. Moore, T. A. Moore, D. Gust, *J. Am. Chem. Soc.* **1995**, *117*, 7202–7212; i) E. Prasad, K. R. Gopidas, *J. Am. Chem. Soc.* **2000**, *122*, 3191–3196.
[30] The rate constant k_{CS} was obtained based on $k_{CS}=1/\tau_{CS}-1/\tau_{o}$, where τ_{CS} denotes the observed decay lifetime of LE bands in **6** and τ_{o} denotes the intrinsic fluorescence decay lifetime of the corresponding monomers **9**.
[31] See the accompanying paper: C.-H. Chen, W.-H. Chen, Y.-H. Liu, T.-S. Lim, T.-Y. Luh, *Chem. Eur. J.* **2011**; DOI: 10.1002/chem.201102031.

Received: July 1, 2011
Revised: August 25, 2011
Published online: December 8, 2011

